Performances and impedance spectroscopy of Small-molecule bulk heterojunction solar cells based on PtOEP: PCBM

A. A. Abuelwafa[a,c *], M. Dongol[a], M. M. El-Nahass[b], T. Soga [c]

[a]Nano and Thin film lab. Physics Department, Faculty of Science, South Valley University, Qena 83523, Egypt.
[b]Physics Department, Faculty of Education, Ain Shams University, Roxy, Cairo 11757, Egypt.
[c]Department of Electrical and Mechanical Engineering, Nagoya Institute of Technology, Nagoya 466-8555, Japan.

Abstract:

Small-molecule Bulk heterojunction (SBHJ) solar cells based on Platinum Octaethylporphyrin (PtOEP) as donor material and [6,6]- phenyl-C61-butyric acid methyl ester (PCBM) as the acceptor were fabricated using spin coating techniques with weight ratios from 1:0.1 to 1:9. The formation of Charge Transfer Complex CTC in the PtOEP: PCBM blend was specified from the redshift of the PtOEP absorption peak after blending with PCBM. The photovoltaic performance for PtOEP: PCBM blends were investigated using the External Quantum Efficiency (EQE) besides the current density-voltage (J-V) characteristics under illumination100 mW/cm^2 (AM1.5G). The BHJ solar cell with PtOEP: PCBM ratio of 1:9 exhibited the best performance. The Impedance Spectroscopy (IS) was examined in the frequency range from 25Hz to 1MHz. The equivalent circuit model was evaluated in details to evaluate the impedance spectroscopy parameters. Dielectric constant ε', dielectric loss ε'' and dielectric modulus were included and discussed in terms of dielectric polarization processes. Dielectric modulus displays the non-Debye relaxation in PtOEP: PCBM BHJ solar cells.

Key words: PtOEP: PCBM; Bulk heterojunction (BHJ); Impedance Spectroscopy; Dielectric Relaxation

[*]***Corresponding author***
e-mail: Amr.abuelwafa@sci.svu.edu.eg (A. A. Abuelwafa)

1. Introduction

Over the past quarter-century, the BHJ solar cells have attracted attention due to their excellent light absorption properties and compatibility with the solution processing technologies enabling new approaches to fabricate cost-effectively. BHJ solar cells represent a unique alternative renewable energy source combining the potential benefits of comparatively low-cost fabrication, flexibility, small weight and wide application through the versatility afforded by appropriate device design [1-6]. Small-molecule(SM) materials have shown unique advantages such as higher charge carrier mobility, purity, in addition to tuning more easily their band structure to absorb sunlight efficiently [7-9]. These advantages make SM BHJ solar cells strong challengers to polymer BHJ solar cells. Hence, it is believed that SM BHJ solar cells are promising to realize their commercial application in the future. Porphyrin and Metalloporphyrins (MTPP) as a typical small organic material molecule, which is a conjugated system consisting of 18π electrons with interesting optical properties, great architectural flexibility, chemical and thermal stability, and has large potential in the field of photovoltaic and molecular photonics as the p-type semiconductors [10-15]. Unique of the best a marketable SM, phosphorescent dye and derivatives of MTPP is the PtOEP which it recently was selected for the electron-donor material in solar cells [15, 16]. One of the effective tools to analyze and understands the electrical properties of thin films and a device such as SBHJ solar cells is the IS technique. It is also a valuable tool to observe bulk and interfacial electrical properties. Also, it used to get information about stability and degradation mechanisms in organic solar cells [17, 18]. Additionally, IS gives access to the dielectric properties of the device. Moreover, it permits the determination of several electronic parameters such as the effective lifetime of the electrons for the recombination process [19] and the mobility [20]. According to the available literature of the photovoltaic and IS of BHJ devices based on PtOEP: PCBM have not been reported yet. Therefore, in detail study is required to investigate the photovoltaic, IS and dielectric properties of PtOEP: PCBM solar cells. The present work we construct the ITO/ PEDOT: PSS/ PtOEP: PCBM/Al solar cells layer with different ratios from PtOEP: PCBM (1:0.1, 1: 05, 1:1, 1:2.5, and 1:9) and study the influence of this ratio on the photocurrent and solar cell performance. Also, in the current study, the IS of our device is investigated and analyzed using the equivalent circuit, which is proposed to model the experimental results and to fit the data. Besides, the dielectric behaviors in the frequency range from 25 to 1 MHz and bias voltage 0.7 V.

2. Experimental techniques

PtOEP (from Sigma-Aldrich) and PCBM (from Nano Spectra) were purchased and used without further purification. The main properties of PtOEP and PCBM **[12-15, 21-23]** are summarized in **Table 1**. The blend solutions of PtOEP: PCBM mixture were prepared by dissolving different weight ratio of the two components (as 1:0.1, 1: 0.5, 1:1, 1:2.5 and 1:9) in 1,2-dichlorobenzene (from Sigma-Aldrich) with a concentration of 20 mg/mL. Solar cells of configuration ITO/PEDOT: PSS/ PtOEP: PCBM /Al (see **Fig. 1(a)**) were fabricated following the procedure clarified in Refs. [24, 25]. The energy level diagram of the fabricated devices and the molecular structure for PtOEP and PCBM are shown in **Fig.1 (b)**. The values of highest occupied molecular orbital (HOMO) and lowest unoccupied molecular orbital (LUMO) for the PtOEP and PCBM, besides the work functions of ITO and Al electrodes were taken from the presented works [25–27]. The optical absorption spectroscopy of PtOEP: PCBM films were carried out using (JASCO V-570) (UV/Vis/ NIR) spectrophotometer. The (EQE) measurements were performed by a single source illumination system (halogen lamp) combined with a monochromator. The J-V characteristics of the devices under white light illumination were determined using standard solar irradiation of 100 mW/cm^2 (AM1.5G) with (JASCO CEP-25BX) spectrophotometer with a cartridge xenon lamp as the light source and a computer-controlled voltage-current source meter (Keithley238) at $25C^o$. The IS was measured at room temperature in the air in the frequency range of 25 Hz to 1M Hz and bias voltage 0.7 V using an impedance analyzer (Agilent 4284A).

3. Results and discussions

Fig 2 shows the normalized absorption of different ratios from PtOEP: PCBM. As shown in this figure the absorption of PtOEP in active layer occurs around 374 nm (Soret (B) band). Also, there are also two transitions called Q bands (Q_1andQ_2) [12] are observed at 547 and 510 nm. While the PCBM absorbs light around the wavelength range of 280-380 nm. It can be seen that with the increase the PCBM concentration in the blends, the absorption peak value of PCBM slowly increases, while the absorption peak value of PtOEP losses, continuously as a result of substituting PCBM with PtOEP. The growth in the PCBM absorption peak value with increasing PCBM concentration is an indication of enhancing in the conjugated lengths in the solar cell active layer. In addition, **Fig. 2** shows that, the absorption spectra of PtOEP: PCBM shifts to the higher wavelength (red shift) with increasing PCBM concentration. The red shift in the PtOEP absorption peak after blending with PCBM molecules (at different ratios) may be attributed to the formation of the CTC from the highest occupied molecular

orbital (HOMO) of PtOEP to the lowest unoccupied molecular orbital (LUMO) of PCBM molecule as a result of a significant interaction between conjugated PtOEP and PCBM molecules in the ground state [25, 28]. The EQE is defined as the ratio of the number of charges extracted out of the device to the number of incident photons. The EQE spectra of the ITO/ PEDOT: PSS/PtOEP: PCBM/Al solar cells with increasing PCBM concentration in the blends are shown in **Fig 3** in the wavelength range from 360 to 650 nm that span the absorption regions of both PtOEP and PCBM. It is clear that the spectral response contains a contribution from both PtOEP and PCBM. It can be seen that the intensity of EQE depends on PCBM weight ratio in PtOEP: PCBM blends. Also, by increasing the PCBM concentration in the PTOEP: PCBM blends the EQE increases entirely and the maximum EQE at 380 nm becomes greater from 7.2 to 10.5%, at PtOEP: PCBM (1:9) sample such significant enhancements in EQE gives rise to an enhanced J_{SC} in devices. The EQE follows the absorption in the wavelength range from 360 to 650 nm. The (J-V) characteristics of the devices under AM1.5G white light illumination (100 mW/cm^2) are shown in **Fig 4.** According to this figure the average device photovoltaic parameters such as open circuit voltage (V_{OC}), short-circuit current density (J_{SC}), fill factor (FF), and power conversion efficiency (PCE, η) for BHJ based on PtOEP: PCBM solar cell at different blend ratios are summarized in **Table2**. It is seen that as the ratio from PtOEP: PCBM is varied from 1:0.1 to 1:9, there is an increasing trend in, V_{OC}, J_{SC}, FF and η up to 1:9 with the increasing PCBM concentration. As shown in **Table 2**, the best results are obtained for the PtOEP: PCBM (1:9) sample, the efficiency (η =0.46%) of which is better than the efficiency of PtOEP: PCBM (1:0.1) (η =0.21 %). Boyd et al [29] reported the co-crystallize of porphyrins with fullerenes and the co-crystallize depend on fullerenes concentration. In our samples, the best efficiency is obtained for the PtOEP: PCBM device with the weight ratio of 1:9, which would be the most favorable for the co-crystallite formation. Also, the best efficiency at the same ratio (1:9) had been observed in the case of ZnTPP: PCBM [30]. Moreover, the enhancement in the photocurrent and solar cell performance with increasing PCBM concentration in the blends may be due to the increase in the interfacial area between donor and acceptor molecules, [31, 32]. The donor materials (PtOEP) in the blend have been developed at an expanding rate, with new design strategies, new building blocks. The efficiency and stability of Organic Photovoltaics (OPV) are very sensitive to the processing conditions, such as the materials used, solvent, solvent additives, annealing, spin coating conditions, etc. [33]. Therefore far, the select of the best condition is still based on a trial-and-error approach. Moreover, problems get up as the OPV technology is translated from the lab-scale to industrial scale, e.g., how to achieve the optimal morphology of a cm^2 device in the industrial scale. Most probably more research has to be carried out

to optimize all the parameters associated with the industrial scale production. The industrial roll-to-roll printing techniques [34] would help minimize the gap between the best efficiency data from lab devices and the large-scale OPV modules. Nowadays OPV will not be able to compete with inorganic solar cells technology in the normal energy production market in the coming 10 years [35], place markets, such as portable electronics chargers, flexible OPV, and wearable PV, are therefore sought in the short term. The IS of all cells with different ratios and the equivalent circuit for PtOEP: PCBM are presented in **Fig. 5**. Every Nyquist plot has a single semicircle, the diameter of the semicircle in impedance spectra obtained depends strongly on the ratios from PtOEP: PCBM. The R_s in this equivalent circuit model is the series resistance of contacts, wires, etc. The single semi-circle (R_p C_p element) describes the charge recombination processes at the PtOEP: PCBM and associated with the diffusion time (τ_d) of carriers across the active layer. R_P corresponds to the R_{rec} (recombination resistance) and C_P is the chemical capacitance. The parameters determined by the fitting of the experimental data are summarized in **Table 2**. The PtOEP: PCBM (1:9) has the lowest values for $R_{S,}$ R_{rec} and (τ_d). The diffusion time can be used to calculate the diffusion coefficient (D) and mobility (μ) using the following relation [18, 36]:

$$D = \frac{L^2}{\tau_d} \quad (1)$$

$$\mu = \frac{eL^2}{k_B T \tau_d} \quad (2)$$

Where, e is the electronic charge, L the thickness of the active layer (˜ 100nm), k_B the Boltzmann constant and T the actual temperature (300K) of the measurements. The values of the diffusion coefficient (D) mobility based on PtOEP: PCBM solar cells are tabled in **Table 2**. The lowest diffusion time (τ_d) value in the PtOEP: PCBM (1:9) solar cell recommends more efficient exciton dissociation at the PtOEP: PCBM interface and a faster charge transport processes, with (D = 4.95×10^{-5} cm^2/sec) and mobility ($\mu = 19.13 \times 10^{-4}$ $cm^2V^{-1}S^{-1}$) which leads to the enhancement of the Jsc and PCE values of the solar cell [19, 36-39]. Therefore, the results of the IS confirmed that the photovoltaic performance for PtOEP: PCBM can be enhanced by increasing PCBM concentration in the active layer. The dielectric studies provide an excellent means to characterize electrical behaviors and valuable information about conduction processes in organic materials. The real Z' and imaginary Z'' parts of the complex impedance (Z) were used for calculation the ε', and ε'', using the following relations [39]:

$$\varepsilon' = \frac{Z''}{\omega C_o (Z'^2 + Z''^2)} \quad (3)$$

$$\varepsilon'' = \frac{Z'}{\omega C_o (Z'^2 + Z''^2)} \quad (4)$$

Where C_o is the vacuum capacitance and given by $\varepsilon_o A/t$, where ε_o is a permittivity of free space. The ε' is related to the capacitive nature of the material and used to measure the reversible energy stored in the material by polarization, while the ε'' is used to measure of the energy required for molecular motion. The frequency dependence of both ε' and ε'' at different ratios from PtOEP; PCBM blends are shown in **Fig. 6(a) & (b).** As observed ε' and ε'' decrease with increasing frequency, this can be explained by means of the dielectric polarization. Therefore, we can explain the decreasing in ε' and ε'' with increasing frequency as follows: The high value of ε' and ε''at low frequency is attributed to space charge and interfacial polarization issued from charge concentrated at the PtOEP: PCBM interfaces. Because, at low frequency, the free charge build up at interfaces within the bulk of the sample [40, 41] and at the interface between the sample and the electrodes. However, with increasing frequency, there was no time for the buildup of charges at the interface, but only for the buildup of charges at the boundaries of conducting species in the material and at the ends of conducting paths [42-44]. The electric modulus formalism is a useful tool to study the relaxation process and electrical transport mechanisms such as carriers hopping rate and conductivity relaxation phenomena [14, 44]. The real M' and imaginary M'' parts of electric modulus were calculated from the impedance data using the relation [44, 45]:

$$M' = \omega C_o Z'' \quad (5)$$

$$M'' = \omega C_o Z' \quad (6)$$

The M' and M'' as a function of frequency at different ratios from PtOEP: PCBM blends are shown in **Fig. 7(a) & (b).** In the low-frequency region, M'values tend to zero, which confirms the negligible or absent electrode polarization phenomenon [14]. A continuous increase in the M' dispersion with increasing frequency and shows a tendency to constant values at high frequencies for all the ratios. This behavior may be due to the short-range mobility of charge carriers [46]. The variation of M'' with frequency is shown in **Fig. 7(b).** It is obvious from this figure that the maximum peak shifted to the higher frequency with increasing the PCBM concentration. The asymmetric broadening of the M" peaks shows that the relaxation of PtOEP: PCBM solar cells was followed the non- Debye type [47, 48].

4. Conclusions

We have fabricated the PtOEP: PCBM BHJ solar cells and studied the effect of PCBM concentration on the photocurrent and performance of the solar cells for the first time. The weight ratios of PtOEP: PCBM were varied from 1:0.1 to 1:9. The CTC was observed in the PtOEP: PCBM blends through the red shift in absorption spectra. The solar cell performance parameters improved with increasing PCBM concentration in the blends. The best results were obtained for the PtOEP: PCBM 1:9, at which the J_{SC}, V_{OC}, FF, and PCE are 1.94 mA/cm^2, 0.53 V, 0.45, and 0.46 %, respectively. IS plot has a single semicircle can be modeled based on an equivalent electric circuit which combination of resistance and capacitance network (joined together in parallel) in series with contact resistance. The smallest values of IS parameters for PtOEP: PCBM (1:9) leads to upgrading in the photocurrent and solar cell performance. The ε' and ε'' are found to decrease with frequency in the investigated ranges. The broad and asymmetric of M'' peaks on both sides of the maxima expected the non-Debye behavior.

References

[1]M. Tang, B. Sun, D. Zhou, Z.Gu , K. Chen , J. Guo, L. Feng, Y. Zhou, Organic Electronics **38,** 213 (2016).

[2] N.Onojima, Y. Ishima, K. Takahashi,Thin Solid Films **615,** 385 (2016).

[3]S. Yamane, Y. Suzuki, T. Miyadera, T. Koganezawa, K. Arai , Y.Akiyama, M. Chikamatsu, Y.Yoshida, H. Suda, J.Mizukado, Sol. Energy Mater. Sol. Cells **151,** 96 (2016).

[4]T. Mahmoudi, S. Seo, H.-Y. Yang, W.-Y.Rho, Y. Wang, Y.-B. Hahn, Nano Energy **28,** 179 (2016).

[5] M.M. Chowdhury, M.K. Alam, Solar Energy **126**, 64 (2016).

[6] Y.Liu,J.Zhao,Z.Li,C.Mu,W.Ma,H.Hu,K.Jiang,H.Lin,H.Ade,H.Yan, Nat.Commun.**5,** 5293 (2014).

[7] J. W. Jung, Dyes and Pigments **137,**512 (2017).

[8] L. Fan, G. Chen, L. Jiang, j. Yuan, Y. Zou, Chemical Physics **493**,77 (2017).

[9] Hongrui Qi, Xiaopeng Xu, Qiang Tao, Youming Zhang, Mengbing Zhu, Weiguo Zhu, Qiang Peng, Yunfeng Liao, Dyes and Pigments 142,406(2017).

[10]T. Liang, L. Xiao, C. Liu, K.Gao, H.i Qin, Y. Cao, X.Peng, Organic Electronics **29** ,127 (2016)..

[11] T.Zhang, M.Liu, Q.Zeng, Z.Wu, L. Piao, S. Zhao, RSC Adv.**3,** 13259 (2013).

[12] A.A. Abuelwafa, A. El-Denglawey, M. Dongol, M.M. El-Nahass, T. Soga, J. Alloy. Compd. **655**, 415(2016).

[13] A.A. Abuelwafa, A. El-Denglawey M. Dongol, M.M. El-Nahass, T. Soga, Optical Materials **49,** 271 (2015).

[14]M. Dongol, M.M. El-Nahass, A. El-Denglawey, A.A. Abuelwafa, T. Soga, Chin. Phys. B **25,** 067201 (2016).

[15] A.A. Abuelwafa, A. El-Denglawey M. Dongol, M.M. El-Nahass, M. S. Ebied,T. Soga, Applied Physics A **124**, 33 (2018).

[16]Y. Shao, Y.Yang, Mater.**17**, 2841(2005).

[17] L. F. Q. P. Marchesi, F. R. Simöoes, L. A. Pocrifka, E. C. Pereira, Phys. Chem. B **115,** 9570 (2011).

[18] B. Arredondo, M. B. M.-López, B. Romero, R. Vergaz, P. R.-Gomez, J. Martorell, Sol. Energy Mater. Sol. Cells **44,** 422 (2016).

[19] W. Aloui, T.Adhikari, J-M.Nunzi, A.Bouazizi, Mater. Res. Bull.**78,** 141 (2016).

[20] G. Garcia-Belmonte, A. Munar, E.M. Barea, J. Bisquert, I. Ugarte, R. Pacios, Organic Electronics **9,** 847 (2008).

[21] M. T. Rispens, A. Meetsma, R. Rittberger, C.J. Brabec, N. S.Sariciftci, J. C. Hummelen, Chem. Commun. **0**, 2116(2003).

[22]G. Paterno, A. J. Warren, J.Spencer, G. Evans, V. G. Sakai, J. Blumbergera , F. Cacialli, J. Mater. Chem. C **1**, 5619 (2013)

[23] A. Lefrançois, B.Luszczynska, B. P.-Donat, C. Lombard, B.Bouthinon, J.-M. Verilhac, M.Gromova1, J. F.Vincent, S. Pouget, F. Chandezon, S. Sadki, P. Reiss, Sci. Rep.**5,** 7768(2015).

[24]Y. A.M. Ismail, N. Kishi, T.Soga, Thin Solid Films **616**, 73 (2016).
[25]Y. A.M. Ismail, T. Soga, T. Jimbo, Sol. Energy Mater. Sol. Cells **94,** 1406 (2010).
[26] B. P. Rand, C.Girotto, A. Mityashin, A. Hadipour, J. Genoe, P.Heremans, Appl. Phys. Lett. **95,** 173304 (2009).
[27] B. P. Rand, S. Schols, D.Cheyns, H. Gommans, C. Girotto , J. Genoe, P. Heremans, J.PoortmansOrganic Electronics **10,** 1015 (2009).
[28] R. R. Zope, M. Olguin, T. Baruah, J. Chem. Phys. **137**, 084317 (2012).
[29] P.D.W. Boyd, C.A. Reed, Acc. Chem. Res. **38,** 235 (2005).
[30] S. M. Khan, M. Kaur, J.R. Heflin, M.H. Sayyad, J. Phys. Chem. Solids **72,** 1430 (2011).
[31] J. Bartelt, Z. Beiley, E. Hoke, W. Mateker, J. Douglas, B. Collins, J. Tumbleston, K. Graham, A. Amassian, H. Ade, J. Fréchet, M. Toney, M. McGehee, Adv. Energy Mater.**3,** 364 (2013).
[32] S. Lan, H. Yang, G. Zhang, X. Wu, W. Ning, S.Wang, H. Chen, T. Guo, J. Phys. Chem. C **120,** 21317 (2016).
[33] K. A. Mazzio, C. K. Luscombe, Chem. Soc. Rev.44, 78 (2015).
[34] A. Abate, J.-P. Correa-Baena, M. Saliba, M. S. Su'ait, F. Bella, Chem. Eur. J.**23**, 1(2017).
[35] S. B. Darling, F. You, RSC Advance. **3**, 17633(2013).
[36] K. Xiong, L. Hou, P. Wang, Y. Xia, D. Chen, B. Xiao, J. Lumine.151 (2014) 193-196.
[37] G. D. Sharma, G. E. Zervaki, P. A. Angaridis, T.N. Kitsopoulos, A. G. Coutsolelos, J. Phys. Chem. C **118**,5968 (2014).
[38]I. Lim, H. T.Bui, N. K. Shrestha, J. K. Lee, S.-H.Han, ACS Appl. Mater. Interfaces **8,** 8637 (2016).
[39] F.F.Muhammad, J Mater Sci: Mater Electron **27,** 637 (2016).
[40] H. Lua, X.Zhang, H. Zhang, J. Appl. Phys. **100,** 054104 (2006).
[41]O. Dhibi ,A. Ltaief, S. Zghal, A. Bouazizi, Vacuum **99,80** (2014).
[42]A. Kyritsis, P. Pissis, J. Polym. Sci. Polym. Phys. **35,** 1545 (1997).
[43] A. Kyritsis, P. Pissis, J. Grammatikakis, J. Polym. Sci. Polym. Phys. **33,** 1737 (1995).
[44] S. B. Aziz, Bull. Mater.Sci. **38,** 1597 (2015).
[45] S. B. Aziz and Z. H. Z. Abidin, J. Appl. Poly. Sci. **132,** 41774 (2015).
[46]A. Tabib, N. Sdiri, H. Elhouichet, M. Férid, Alloy. Compd. **622,** 687 (2015).
[47] F.S. Howell, R.A. Bose, P.B. Macedo, C.T. Moynihan, Phys. Chem. **78,** 639 (1974).
[48] S. Hajlaoui, I. Chaabane, A.Oueslati, K. Guidara, Physica B **474**, 90 (2015).

Figure caption

Fig. 1. (a) Schematic view of PtOEP: PCBM device architecture and (b) Schematic diagram of the energy levels in the PtOEP: PCBM solar cells

Fig. 2. Normalized absorption spectra of PtOEP: PCBM solar cells. .

Fig. 3. EQE spectra of the ITO/PEDOT: PSS/PtOEP: PCBM/Al solar cells.

Fig. 4. J–V characteristics of PtOEP: PCBM solar cells.

Fig. 5. Nyquist plots of PtOEP: PCBM solar cells. The inset shows the basic RC model of the equivalent circuit.

Fig. 6. The frequency-dependent (a) ε' and (b) ε'' for PtOEP: PCBM solar cells.

Fig. 7. The frequency-dependent (a) M' and (b) M'' for PtOEP: PCBM solar cells.

Table caption

Table 1. Summary of main properties for PtOEP and PCBM **.**

Table 2. Summary of device parameters of BHJ solar cells based on PtOEP: PCBM **.**

Figures

Fig. 1.

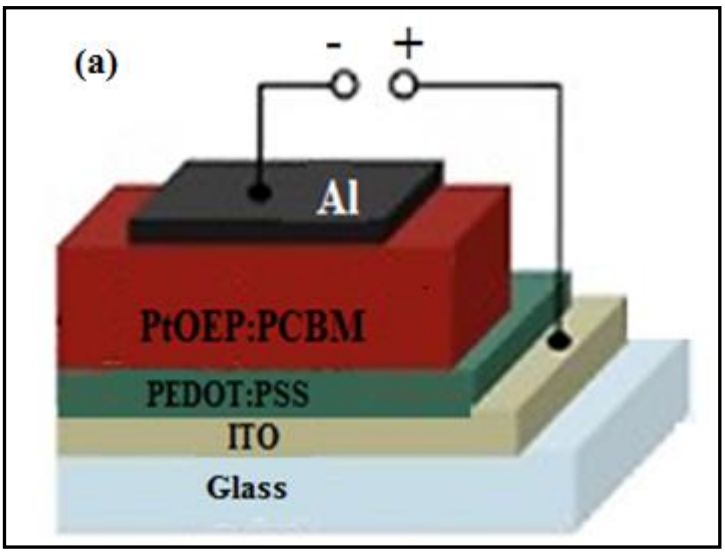

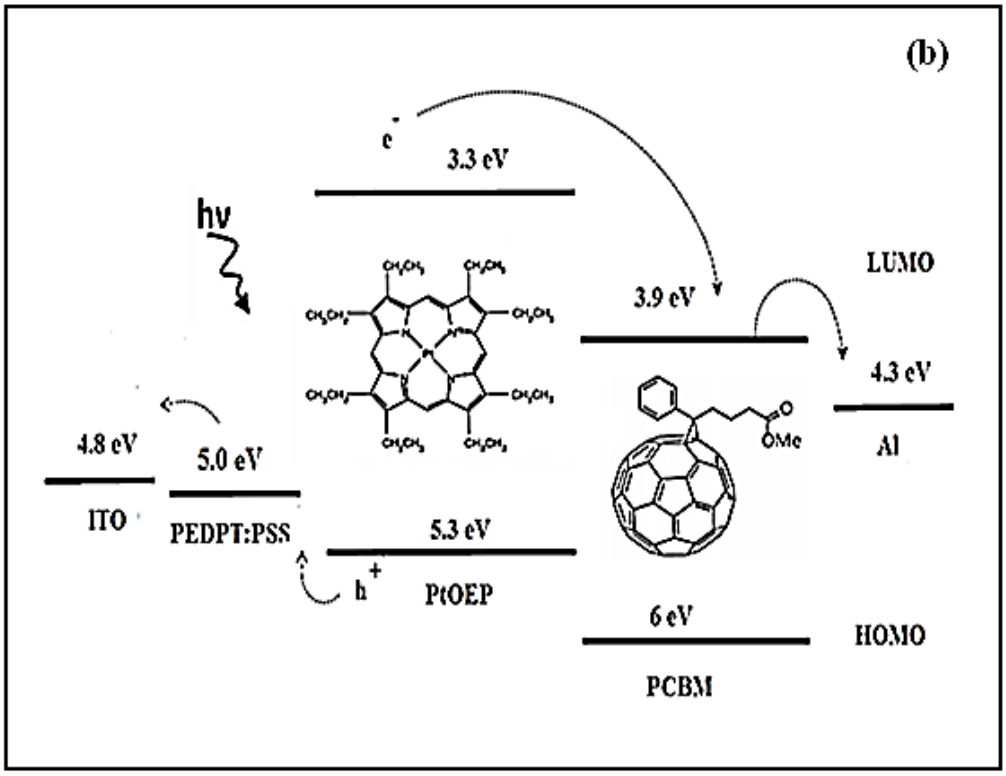

Fig. 2.

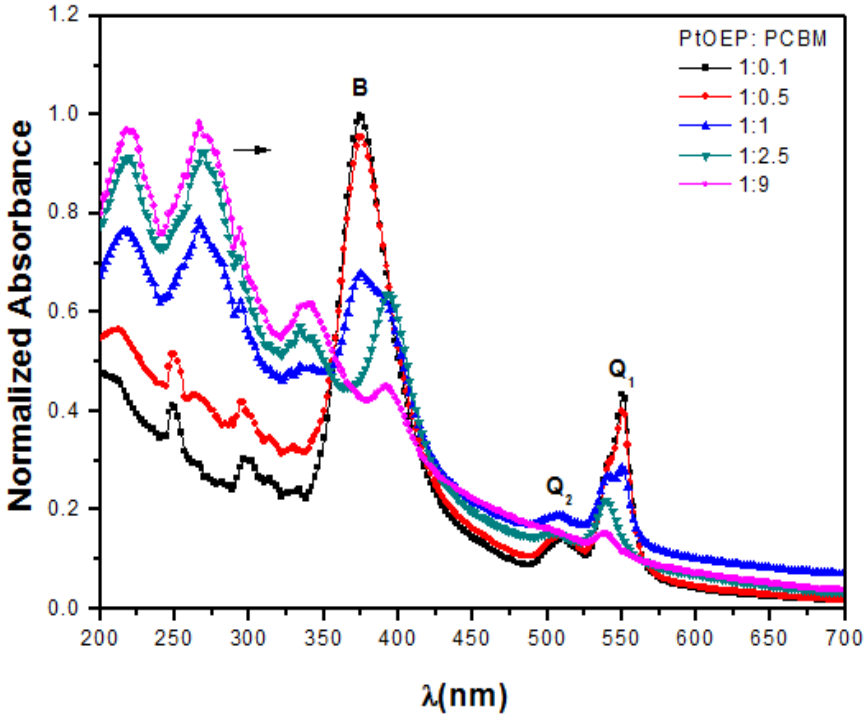
PtOEP: PCBM
1:0.1
1:0.5
1:1
1:2.5
1:9
B
Q1
Q2
Normalized Absorbance
λ(nm)

Fig. 3.

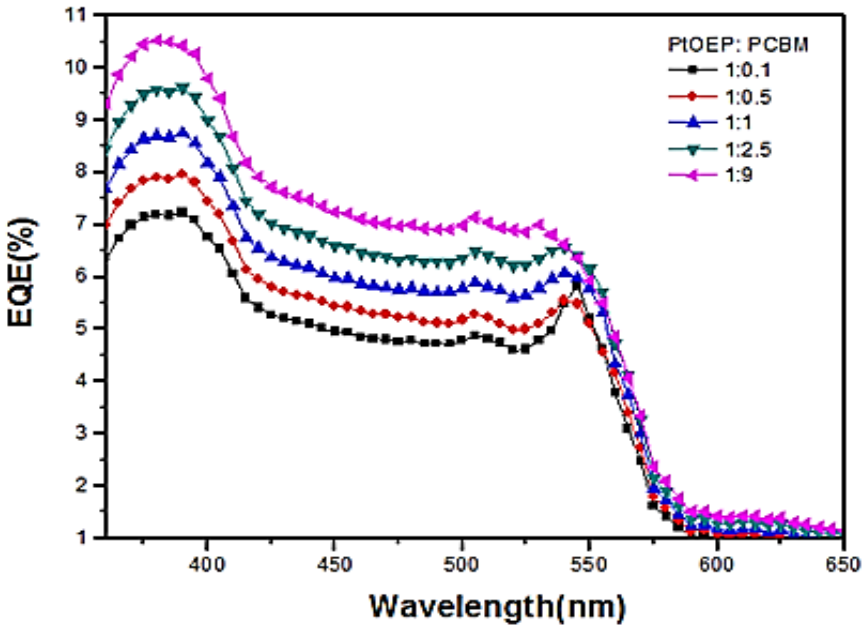
PtOEP: PCBM
1:0.1
1:0.5
1:1
1:2.5
1:9
EQE(%)
Wavelength(nm)

Fig. 4.

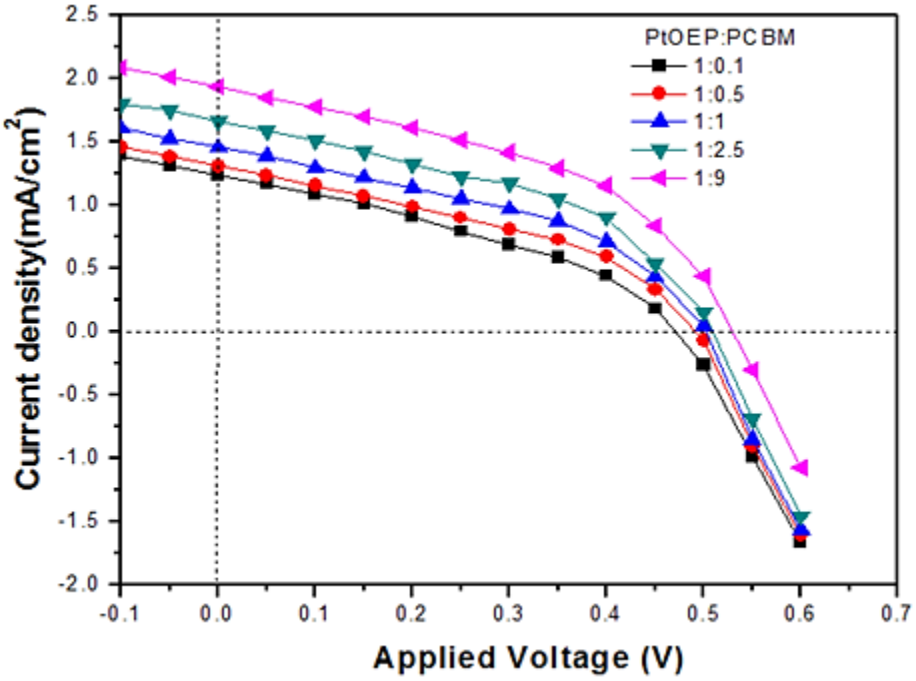
PtOEP:PCBM
1:0.1
1:0.5
1:1
1:2.5
1:9
Current density(mA/cm^2)
Applied Voltage (V)

Fig. 5.

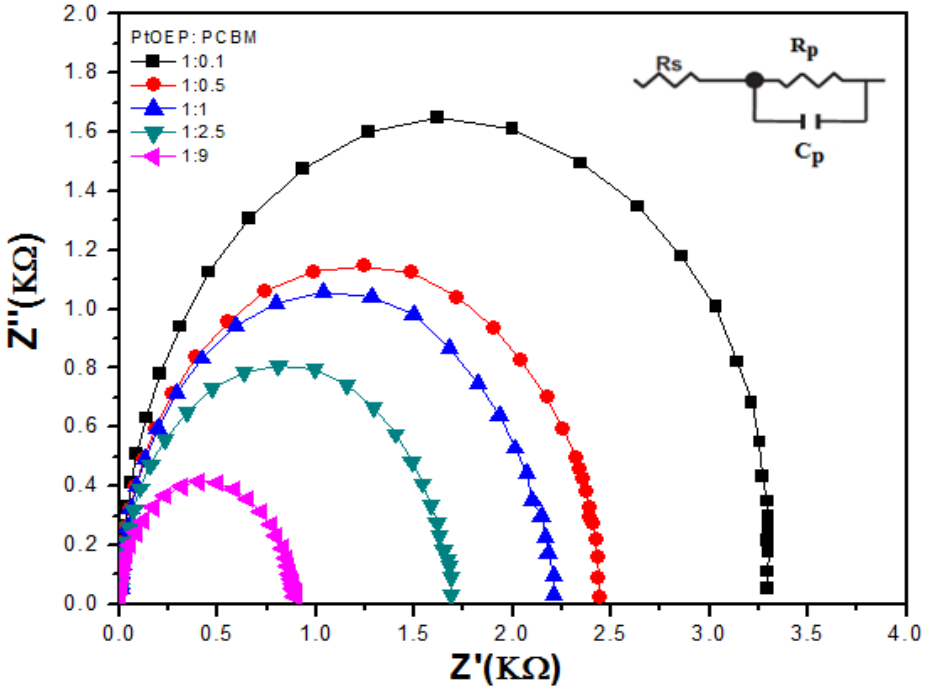
PtOEP: PCBM
1:0.1
1:0.5
1:1
1:2.5
1:9
Rs
Rp
Cp
Z''(KΩ)
Z'(KΩ)

Fig. 6.

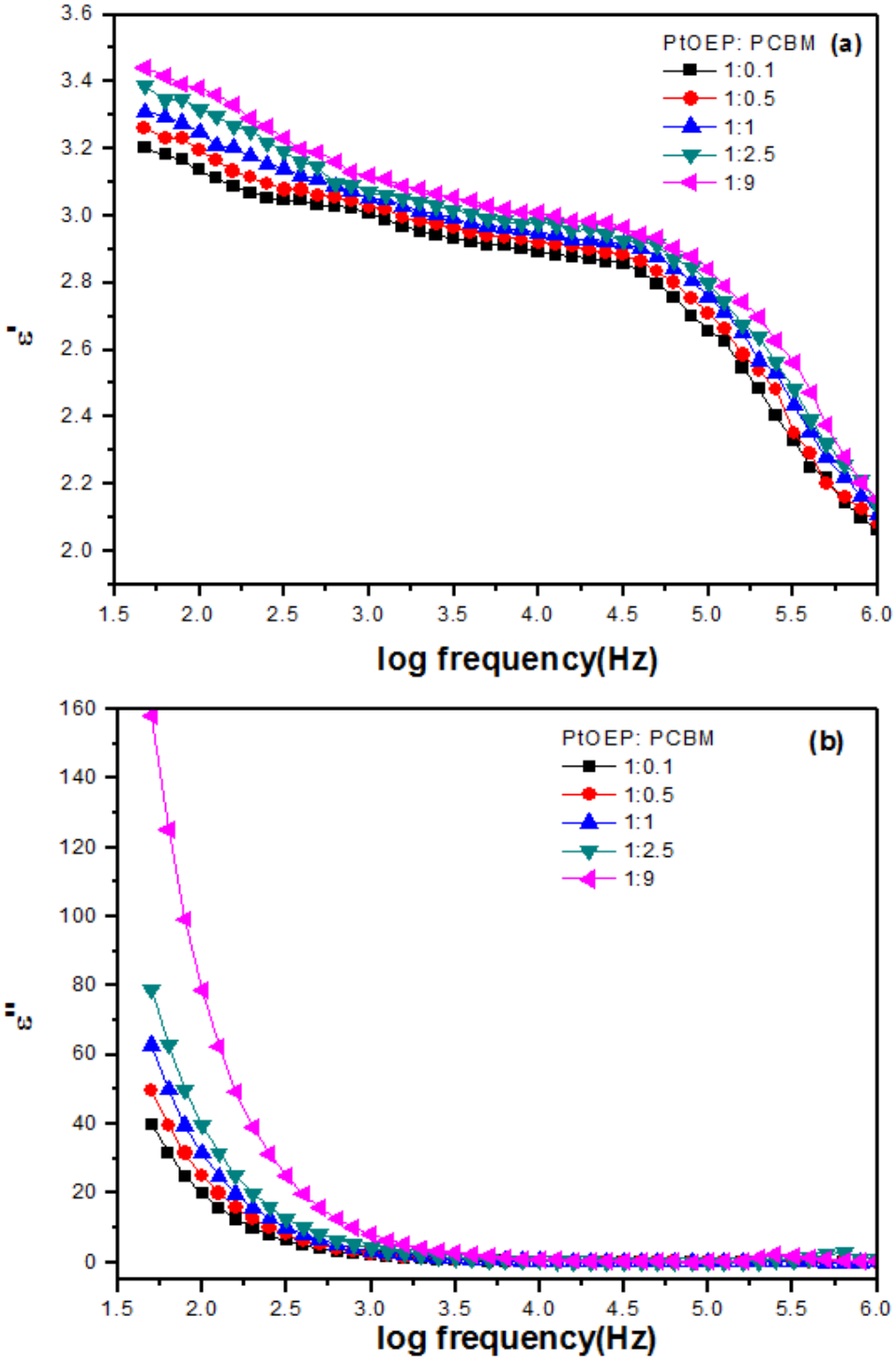
PtOEP: PCBM (a)
1:0.1
1:0.5
1:1
1:2.5
1:9
ε'
log frequency(Hz)
PtOEP: PCBM (b)
1:0.1
1:0.5
1:1
1:2.5
1:9
ε''
log frequency(Hz)

.

Fig. 7.

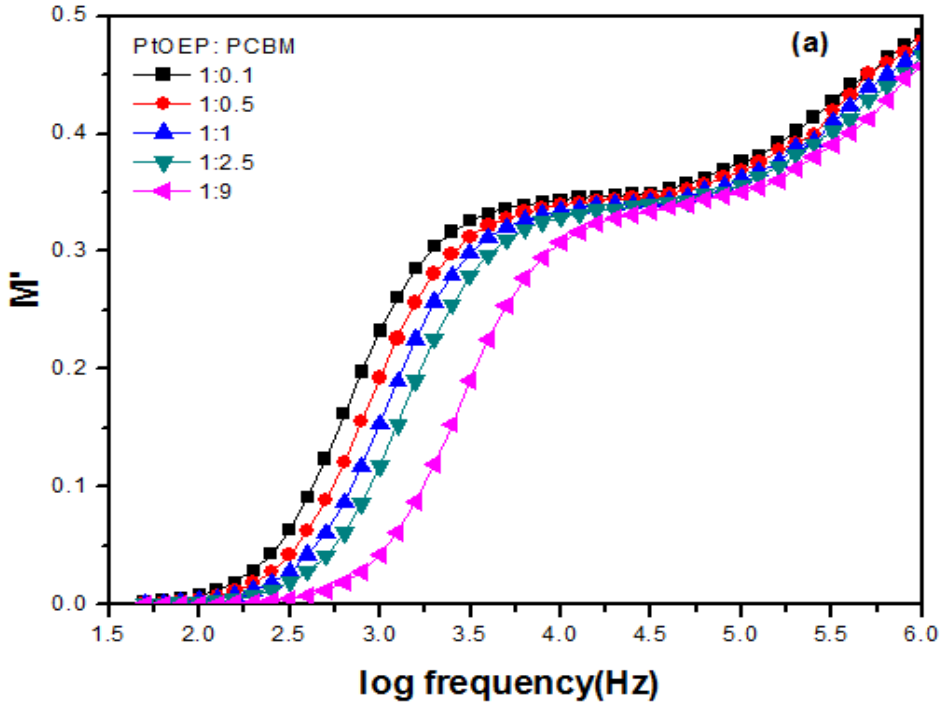
PtOEP: PCBM
1:0.1
1:0.5
1:1
1:2.5
1:9
(a)
M'
log frequency(Hz)

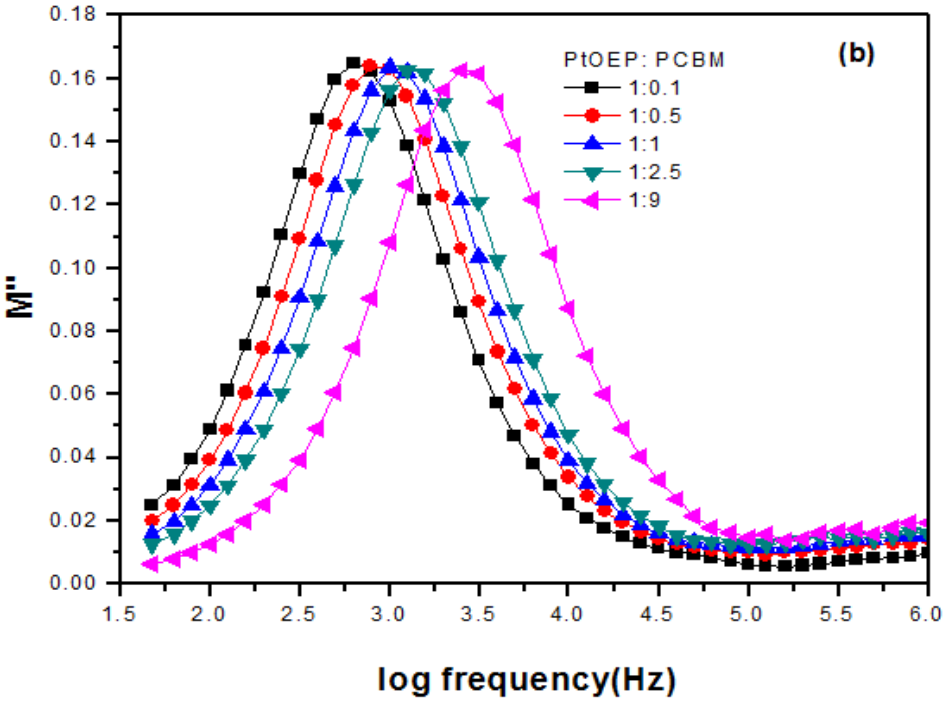
PtOEP: PCBM
1:0.1
1:0.5
1:1
1:2.5
1:9
(b)
M"
log frequency(Hz)

Table.1

Main properties	PtOEP	PCBM
Empirical formula	$C_{36}H_{44}N_4Pt$	$C_{72}H_{14}O_2$
Molecular weight (g/mol)	727.8	910.88
Crystal color	Red	Brown
Density (g/cm^3)	1.61	1.72
Crystal system	Triclinic	Monoclinic
Space group	$P\bar{1}$	P2(1)/n
Unit cell	a=8.193Å, b= 10.033 Å , c=10.059Å ,α=84.53°,β=80.95°,γ=67.15°	a=13..47, b= 11.1 Å , c=19.09Å ,α=90°,β=106.9°,γ=90°
The unit cell volume(A^3)	752	3708.70
Semiconductor Type	P-type	N-type

Table.2

PtOEP : PCBM Ratios	V_{OC} (Volt)	J_{sc} (mA/cm^2)	FF	η%	R_S (Ω)	R_p (Ω)	τ_d x10^{-5} (sec)	Dx10^{-5} (cm^2/sec)	μ x10^{-4} (cm^{2}V^{-1}S^{-1})
1:0.1	0.47	1.24	0.35	0.21	21.4	3283.6	7.96	1.25	4.85
1:0.5	0.49	1.31	0.39	0.25	14.8	2433.4	6.36	1.57	6.07
1:1	0.5	1.46	0.42	0.31	12.6	2199.8	5.04	1.98	7.66
1:2.5	0.51	1.66	0.43	0.37	7.2	1681.5	3.98	2.51	9.71
1:9	0.53	1.94	0.45	0.46	5.1	889.6	2.02	4.95	19.13